



Effectiveness of blended modified biomaterials and coagulants in removing heavy metal ions from drinking water before determination by ICP-OES

David Obasi Igwe^{*a}, Chukwunonso Peter Okoli^b, George C. Mbaeyi^c, Omaka Omaka Ndukaku^a, and Aka Beatrice Lebechi^c

^aDepartment of Chemistry, Alex Ekwueme Federal University, Ndufu-Alike, Abakaliki, Ebonyi State.

^bDepartment of Mathematics and Statistics, Alex Ekwueme Federal University, Ndufu-Alike, Abakaliki, Ebonyi State.

^cDepartment of Chemistry, University of Agriculture and Environmental Sciences, Umuagwo, Imo State,

ARTICLE INFO:

Received 19 Oct 2024

Revised form 16 Jan 2025

Accepted 10 Feb 2025

Available online 28 March 2025

Keywords:

Dissolved Heavy Metals,
 Inductively coupled plasma optical emission spectroscopy,
 Biomaterial,
 Scrap Iron,
 River water,
 Borehole Water

ABSTRACT

The effectiveness and characterization of blended composite materials made of modified biomaterials and iron (III) sulfate coagulant to remove selected dissolved heavy metals from water-chosen samples were determined during the rainy and dry seasons by inductively coupled plasma optical emission spectroscopy (ICP-OES). Water samples were mechanically batch agitated at their prevailing pHs with optimal composite doses. Following the treatment during the rainy season, the results indicated a percent elimination range of 62.16-99.19 percent. Cu > Zn > Pb > Cd; Zn > Cu > Pb > Cd; Pb > Cu > Cd > Zn; and Zn > Cu > Cd > Pb were the percent removal trends in the Funai borehole water (FBW), Assemblies of God church borehole water (ABW), Ebonyi River water (EBRW), and Eziyiaku river water, Akaeze (ERWA) samples, respectively. During the dry season, a removal range of 93.70 – 100 percent was recorded in all samples. Concentrations of all residual metals except Cd satisfied the World Health Organization and Nigerian Standard Organization permissible levels. Interactions of the variables at ($p < 0.05$, $p < 0.01$, and $p < 0.001$) indicated a statistically significant difference. The reduced linear model of analysis of variance (ANOVA) and response surface methodology employed to predict the responses of main and interaction effects of variables for the dosage optimization of composite materials indicated suitability and statistical significance.

1. Introduction

The increasing population with industrialization has been implicated in impacting significantly environmental pollution with chemical compounds, with surface water and groundwater increasingly becoming sinks for heavy metal ions. Mining activities have contributed significantly to water pollution with dissolved heavy metals in recent years

[1]. Household waste, discarded electronic devices, and industrial solid wastes dumped indiscriminately have also contributed to trace metal pollution of water bodies [2]. Furthermore, heavy metal poisoning of water supplies has been linked to the overuse of herbicides, pesticides, and fertilizers. Heavy metals have been found in various thick laminated leaves used to cover food products like *eba*, *moi-moi*, and *agidi*, according to [3]. The leaves degrade due to heavy precipitation and runoff; the released heavy metals enter rivers and percolate into aquifers,

*Corresponding Author: David Obasi Igwe

Email: digwe53@yahoo.com

<https://doi.org/10.24200/amecj.v8.i01.378>

poisoning water bodies. The authors also implicated small-scale road-side mechanics and petroleum motor spirit road-side traders, sometimes known as “black marketers,” in the pollution of the environment with heavy metals. Water contamination is also caused by the dissolution of heavy metal-containing rocks and soils and bush burning [4]. Chemical elements with a specific gravity of at least 5 times that of water are known as heavy metals. They are neither biodegradable nor biodegradable in environmental matrices. Mercury in water was determined using multiwall carbon nanotubes [5]. They can be found in colloidal, particulate, and dissolved forms in surface waters, but their concentrations are typically modest [5, 6]. According to Misihairabgwi et al. [7], colloidal and particulate phases may occur as hydroxides, oxides, silicates, or sulfides; or absorbed into clay, silicate, or organic matter, while the dissolved phase is in the form of ions or unionized organometallic chelates or complexes [3]. As much as some of these heavy metals (e.g., copper, cobalt, iron, manganese, molybdenum, vanadium, strontium, selenium, and zinc) are essentially needed in very low levels in the human body to maintain metabolism when their concentrations in drinking water are above the threshold limit, they become poisonous. Because they build up in living tissues, they can cause disorders including neurological and renal breakdown, brain damage, high blood pressure, convulsions, cancer, metabolic acidosis, and mouth ulcers, among others [6, 7, 8]. linked these heavy metals’ toxicity to developing complexes in human cells with organic molecules containing oxygen, sulfur, or nitrogen groups. Some enzymes are inactivated, protein structure is altered, cells lose their capacity to function normally, or cells die [6, 9]. Children are more susceptible to heavy metal toxicity than adults, particularly when exposed to lead poisoning, due to their faster rate of absorption. According to [9,10], the toxicity of these metal ions is determined by their stability, bioavailability, and environmental mobility, as well as the speciation, concentration, and type of heavy metal. Due to epileptic power supply, lack of maintenance culture, and high operational expenses, governments and donor agencies’ efforts to solve

potable water scarcity for 3 million Ebonyians never achieved any positive outcomes, according to [11]. As a result, drinking water is not properly treated, treatment plants are under-equipped or moribund, and distribution pipes are broken, causing regrowth. Neuropsychological effects of long-term exposure to heavy metal reported by Bagheri et al. [12]. According to [11], the demand for water in Ebonyi State has increased due to the growing population, and people are now sourcing their drinking water from boreholes, hand-dug wells, streams, and rivers. Ebonyi State is endowed with large deposits of heavy metals. However, the rate of accumulation of these heavy metals into the water bodies in virtually all three senatorial zones of the State due largely to the mining of these solid minerals and discharge of the untreated effluents has become a serious health concern, especially to natives who source their drinking water from these water bodies [13]. Many poor countries are increasingly interested in developing water treatment techniques that can efficiently and affordably remove heavy metal ions from drinking water [14]. Membrane filtration (candle, packed column, or beds) [15] ion exchange, reverse osmosis, solid-liquid trap phase extraction, and solid-phase microextraction [16, 17], as well as gas field separation consolidation process [18], are not cost-effective for use in treating water in the developing countries. Electrodialysis, or chemical precipitation, to treat water at home is costly, especially if the volume of water is large. In addition to incomplete removal at low metal levels, the operations are difficult for non-skilled users. In multi-metals systems, studies have demonstrated that single strategies of heavy metal removal, such as adsorption using activated carbons, are challenged by interaction effects and competition for adsorption sites, lowering the removal effectiveness of one heavy metal over the others [19]. The present study used different blends of modified biomaterials and coagulants to absorb selected heavy metals in water samples naturally containing multi-metal cations. The choice allowed interaction effects and competition for sites on the modified biomaterials to be avoided through the synergic effects of charge

separation and sweep flocculation. This method has advantages over the traditional methods in that the precursor materials are abundant locally (from local markets and refuse dumpsites), sustainable, require unskilled operators, cost-effective, and accessible to rural dwellers. Nevertheless, the potential shortcoming of this method lies in the fact that the recommended optimum dose of the different blended composites used in this present study might fall short of the required dose if the level of pollution of the river and borehole waters increases for increased anthropogenic activities and vice-versa. Information abounds in the literature concerning the pollution of the major water resources (Ebonyi River and Ezeiyaku River, in Ebonyi North and Central, and Ebonyi South senatorial zones, respectively, and groundwater) by heavy metals as a result of the mining of lead, zinc ores, and other metal ores in all the senatorial zones of Ebonyi State. Nevertheless, besides the works of Igwe *et al.* [20, 21], there is a dearth of information regarding efficient techniques for the removal of pollutants such as heavy metals, which can be affordable to the economically less privileged Ebonyians, who depend on these water sources for drinking and other domestic purposes, especially in the rural areas.

Therefore, the current study created a composite material using local sodium chloride-activated carbon derived from coconut shell, counter softwood, and iron(III) sulfate derived from scrap iron metal and evaluated its potential in the removal of heavy metals (HMs), notably lead (Pb), cadmium (Cd), mercury (Hg), and nickel (Ni), from borehole and river samples (through a multi-barrier treatment strategy).

2. Experimental

2.1. Instruments

The following instruments were used in this study: muffle furnace (carboniser) supplied by the Industrial Chemistry Department, Ebonyi State University, Abakaliki, pH meter (LF 90, Germany), Benchtop pH Meter, Orion Star A221 pH Portable Meter, labtech digital turbidity meter (probe), SEM (Phenom-Prox, Phenom world Eindhoven the Netherlands) and EC meter (WKW, Germany). Others include TDS Meter

(CD650, ELUTECH Instruments), Micromeritics ASAP 2020 Surface Area and Porosity Analyzer: Norcross (GA 30093-2901, U.S.A.), ICP-OES (Perkin Elmer 8000 ICP-OES), and FOV (537 μm , Mode: 15kV - Image, Detector: BSD Full DSM 9872 Gemini SEM) were used.

2.2. Reagents

The chemicals used in this study were of analytical grade, which includes acetone (Hainan Starry, CAS N: 67-64-1, China), concentrated sulphuric acid (Merck Millipore, CAS N: 7664-93-9, Darmstadt, Germany), hydrochloric acid (Merck Millipore, CAS N: 7647-01-0, Darmstadt, Germany), and Hydrogen peroxide (JIGS Chemical, CAS N: 7722-84-1, India). Others are copper sulfate (Spectrum Chemical, CAS N: 7758-99-8, New Jersey, USA), Iodine (Merck Millipore, CAS N: 7553-56-2, Darmstadt, Germany), Sodium thiosulphate (Sigma Aldrich, CAS number 7772-98-7, Massachusetts), Sodium hydroxide (Sigma Aldrich, CAS N: 1310-73-2, Massachusetts), and Potassium chloride (Sigma Aldrich CAS N: 7447-40-7, Massachusetts). Some of materials such as Granulated coconut shell carbon (GCSC), Akparata (counter)softwood carbon (ACSC), and Iron(III) sulphate coagulant (ISC) were prepared. The major drinking water sources in Ebonyi State are borehole water (motorized and mechanical) and surface water (rivers and streams). Therefore, water samples were taken at the Ebonyi River and Ezeiyaku River, precisely at Mgbo and Ndiachi Akaeze, in Abakaliki and Ivo local government areas of Ebonyi State. The locations were chosen due to the heavy settlement of locals along these rivers. Alex Ekwueme Federal University, Ndufu-Alike, and Assemblies of God Church Avenue, Abakaliki, were selected for borehole water sampling due to the use of these waters for cooking/drinking by students and inhabitants in the capital city, Abakaliki, respectively. The sampling was carried out in August, September, and October 2022, representing the rainy season, and December 2022, January, and February 2023, representing the dry seasons.

2.3. Study area

Abakaliki, AEFUNAI Ikwo, and Akaeze are in

Ebonyi State's North, Central, and South Senatorial Zones, respectively. Mgbo is located on longitude 80° 15' E and Latitude 60° 22' N, Assemblies of God Church Avenue is situated on Longitude 80° 10' E and Latitude 60° 20' N. AE-FUNAI is on Longitude 80° 17' E and Latitude 60° 8' N, while Ndiachi, Akaeze is located on Longitude 70° 45' E and Latitude 50° 55' N [21]. The study areas are defined by two distinct seasons: the dry season (November to March) and the rainy season (April to October) [21]. The rainy season peaks between July and August. Cretaceous sedimentary rocks underlie the Albian Esu River and Turonian Eze-Aku Formations in the three research locations. The lithology of Abakaliki (containing Abakaliki urban and Ikwo) is highly folded, faulted, and fractured by tectonic activity [22]. Dark grey shale, volcanoclastics, mudstone, manganese sandstone, siltstone, and limestone comprise most of the rock [23]. In the geology of the study areas, especially Abakaliki and Ikwo [24], there is a significant deposit of lead-zinc mineralization, Galena (PbS) and Sphalerite (ZnS) veins, and this occurrence in the fracture led to mining activities along the hydrothermal Pb-Zn vein lodes. Groundwater availability in Abakaliki and Ikwo is inadequate due to underlying shale or aquiclude and limited groundwater recharge. According to [25], the geology of the Abakaliki basin is characterized by compressional tectonic pressures, resulting in low primary porosity, which indicates slow movement. The Esu River facies are notable for insufficient water recharge [26]. Only the Eze-Aku and Agwu formations in the Esu River, Eze-Aku, Agwum Nkporo, and Mamu formations in the Cross River basin are suitable aquifers [21]. The Turonian Eze-Aku group comprises substantial grey and black calcareous shale, limestone, and siltstone. The principal shale unit of this group has its kind of locality near the Eze-aku River in Akaeze.

2.4. Sample collection

The water samples were collected using conventional procedures. Plastic bottles (1 liter) were washed in warm liquid soap, rinsed thoroughly with warm de-ionized water, and then immersed for 48 hours in 10

% nitric acid [27]. They were then thoroughly cleaned in de-ionized water and securely protected. To obtain representative samples, the motorized borehole taps were allowed to run for 5 minutes, after which the bottles were cleaned 3-4 times before collecting three replicate samples by 7:20 a.m. The river was agitated with the sample bottle at the sampling point (banks and center of the river), then uncapped and rinsed three times with the water sample before plunging about 30 cm below the water's surface.

2.5. Activated carbon preparation and synthesis of iron (III) sulfate

2.5.1. Coconut shell and Akparata counter softwood modification and pyrolysis

Different masses (of impregnation ratios of 1:1, 1:2, 1:3, and 2:1) of the coconut shell and *akparata* (counter) softwood were soaked with the local sodium chloride solution and boiled until the mixture became pasty [20, 21]. They were filtered and dried in an oven for 2 hours, after which they were carbonized using a muffle furnace between the temperature range of 450 and 650 °C. The activated biomaterials were washed thoroughly with distilled water and dried in the oven (Gen lab) for another 2 hours before use.

2.5.2. Preparation of coagulant and adsorbent

The coagulant was made using the [20, 21] method. A 23.5 g scrap iron metal was first degreased and soaked in 2 liters of 40 % concentrated sulphuric acid in a capped amber bottle and was allowed to react for 24 hours. The resulting iron (II) sulfate crystals were removed, washed with enough distilled water, and crushed to a fine size. Oxidization of the iron (II) sulfate crystal was done by careful addition of 30 – 40 % hydrogen peroxide solution in the presence of 10 mg per 50 mL of copper sulfate as a catalyst at a temperature of 80 °C in 500 mL beaker using temperature, and time regulated magnetic hot-plate stirrer until a brownish yellow paste was formed. It was allowed for about 3 hours for complete oxidation to iron (III) sulfate. The iron(III) sulfate paste was then dried in the oven at 120°C for 2 hours. An iron (III) sulfate lump formed and was then ground into anhydrous powder.

2.6. Characterization of GCSC, ACSC and ISC

2.6.1. Degree of pore development (DPD)

The iodine test assessed the DPD distribution using the Igwe *et al.* [20] technique. A 1.0 g of the different impregnated ratios of the GCSC and ACSC was separately wetted with 5 ml of 5 % w/v of concentrated hydrochloric acid and mechanically shaken in a 100 ml conical flask. This was stirred for 1 hour with 25 ml of 0.1 M iodine solution in a magnetic stirrer; the mixture was then filtered. A standardized 0.1 M sodium thiosulphate solution was titrated against 25 mL of the filtrate to a cloudy solution using starch solution as an indicator. The iodine values of the different impregnated biomaterials were obtained using Equation 1.

$$\text{DPD } (X_m) = \frac{[M_i \times 126 \times V_i] - (V_i + V_A/V_F \times (M_T \times 126.93) V_T]}{W_{MB}} \quad (\text{Eq. 1})$$

In equation 1, V_i is the volume of iodine solution added to the flask, V_A is the volume of 5 % HCl used, M_i is the molar concentration of the iodine stock solution, V_T is the volume or average titre of the thiosulphate solution, W_{MB} is the weight of the adsorbent, and X_m is the adsorbent's iodine number in mg g^{-1} . VF is the volume of filtrate used. M_T and V_T are thiosulfate molar concentration and volume or average titer, respectively.

2.6.2. Surface charges of GCSC, ACSC and ISC

The approach of [21] was used to make this determination. With 0.1 M NaOH and HCl solutions, seventeen sets of 100 ml beakers containing 50 mL of 0.1 M potassium chloride (KCl) solution with initial pH values ranging from 2.00 to 10.00 were prepared. 0.150 g of adsorbents and 0.002 g of coagulant were soaked individually in the initial pH of KCl solutions for 48 hours to achieve equilibrium. The ultimate pH values of the various contents of the beakers were evaluated after two days.

2.6.3. Surface morphology of the GCSC and ACSC

For surface and morphological characterization, a scanning electron microscope (SEM) (Phenom-Prox, Phenom-World Eindhoven, the Netherlands) was used.

2.6.4. Elemental composition of the GCSC and ACSC

Energy Dispersive X-ray (EDX) was employed to characterize the ultimate analysis of the biomaterials.

2.7. General procedure

The procedure is followed by [schema 1](#). During the rainy and dry seasons, a 250 mL sample of Funai borehole water (FBW) was batched separately and mechanically agitated with five sets of GCSC/ACSC/ISC composite materials masses (0.500, 0.500, and 0.005; 0.500, 1.000, and 0.010; 1.000, 0.500, and 0.015; 1.500, 0.500, and 0.020; 0.500, 1.500, and 0.025; 2.000, 2.000, and 0.030) to determine the optimum dose of the composite treatment materials needed for the removal of DHMs in the water samples. At the water sample's prevailing pH, each mix was physically stirred for 60 minutes before sedimentation. After filtering the untreated and treated FBW water samples, the concentrations of the untreated and treated FBW water samples were determined using an inductively coupled plasma optical emission spectrophotometer (Perkin Elmer 8000 ICP-OES) [28]. The optimal doses treated the other water samples during both seasons. The water samples were treated using the same procedure as the optimization process. The percentage of DHMs removed from the water samples was estimated using Equation 2.

The rationale behind the choice of the specific combinations of the blended composite materials was based firstly on the information obtained from past studies that modified coconut shell carbon is rigid (in terms of abrasion resistance) and effective in adsorbing contaminants in aqueous system (in terms of low macroporosity and high carbon yield)

$$\% \text{ Removal} = \frac{\text{Conc. of DHMs in untreated sample} - \text{Conc. of DHMs in treated sample}}{\text{Conc. of DHMs in untreated sample}} \times 100 \quad (\text{Eq. 2})$$

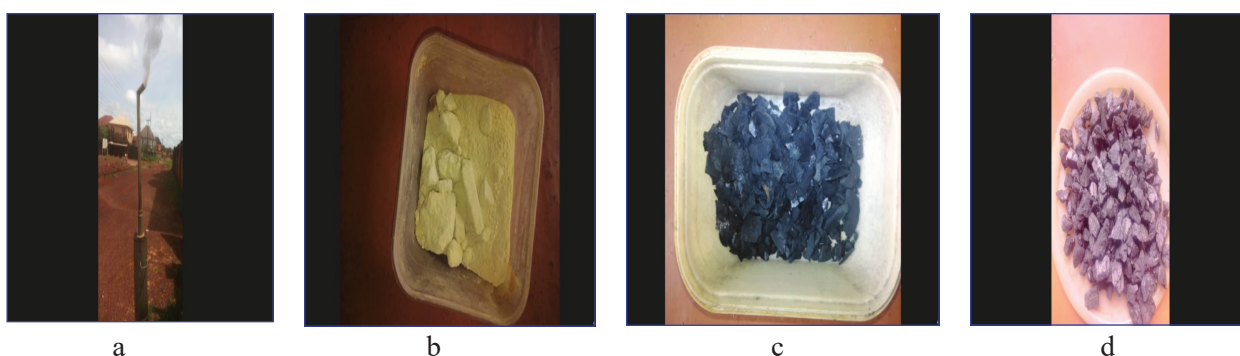
[29]. Furthermore, modified coconut shell carbon contains more micropore distributions, while modified wood carbon contains more mesopore/macropore distributions [30]. By combining these different adsorbents, the effectiveness of removing both small and large size-cations contaminants in the water samples would have been enhanced. Secondly, since the medium from which the DHMs are being removed is a multi-component metal system that has shown to present competition amongst the different size cations during adsorption, the inclusion of the third component-the iron(III) sulphate coagulant-synergistically removes any recalcitrant adsorbate by neutralization and sweep-floc mechanisms due to the high density of its floc formed [31].

3. Results and discussion

3.1. The impact of modification of GCSC and ACSC on the pore development (iodine test)

Table 1 presents the values of the iodine test carried out to determine the extent of pore development on the surface of the GCSC and ACSC. Table 1 indicated that the iodine values for the GCSC and ACSC at different impregnation ratios ranged from 1204 to 1613 and 1115 to 1532 mg/g, respectively. The lowest values were observed with an impregnation ratio of 3:1. It can be inferred from Table 1 that the iodine values obtained for

ACSC at the different impregnation ratios at 500 C were lower than the corresponding iodine values for GCSC. This may be attributed to the different types of precursor biomaterial containing various degrees of cellulose and hemicellulose. An increase in a biomaterial's cellulose and hemicellulose content has been observed to impart a higher degree of microporosity when activated [32]. It was equally observed that increasing the impregnation ratio resulted in increased iodine values of the biomaterials up to a 2:3 impregnation ratio for both GCSC and ACSC. The highest iodine values obtained at an impregnation ratio of 2:3 for both adsorbents were 1613 and 1532 mg g⁻¹. At a 0.3 impregnation ratio, the activating agent penetrated the inner structure to widen the pores. This increase in iodine value with an increase in impregnation ratio reached its plateau at an impregnation ratio of 0.7. This is due to the extensive dehydration and catalytic actions of the alkali metal (Na, the activating agent) on the cellulose and hemicellulose components of the adsorbent [33]. Further, an increase in the impregnation ratio resulted in the excessive carbon burn-off and collapse of carbon structure as well as a reduction in the surface area of both GCSC and ACSC due to micropores transition to mesopores and macropores [34] and at the impregnation



Schema 1. Muffle furnace (a) used prepared iron(III) sulphate coagulant from scrap iron (b), granulated activated coconut shell carbon (c), and counter wood carbon (d).

Table 1. Iodine Value Test for the Modified Biomaterials, Iodine Value (mg g⁻¹)

Impregnation Ratio	1:3	1:2	2:3	1:1	2:1	3:1
GCSC	1306	1489	1613	1383	1351	1204
ACSC	1287	1441	1532	1310	1286	1115

ratio of 3, the lowest iodine values for the two adsorbents were achieved.

Table 2 presents the results of the characteristics of the water samples. The mean values of the TDS and EC for the untreated water samples recorded during the rainy and dry seasons (Table 2) showed that the highest mean values (43.05 ± 0.17 , and 72.61 ± 0.20 ; 113.55 ± 0.11 , and 206.41 ± 0.16) were observed in FBW samples while the highest mean pH values (8.01 ± 0.16 , and 8.05 ± 0.12) were observed in Assemblies of God church borehole water (rainy season) and FBW (dry season), respectively. After treatment, the highest mean TDS and EC values obtained (31.73 ± 0.22 and 5.35 ± 0.05 ; 84.90 ± 0.30 , and 41.62 ± 0.09) were observed in FBW samples for both seasons, while 7.64 ± 0.08 , and 7.42 ± 0.25 mean pH values were recorded for ABW and FBW samples, respectively. Total dissolved solids (TDS) measure all the dissolved cations and anions, including carbonates, chlorides, sulfates, nitrates, sodium, potassium, calcium, and magnesium [35]. The results indicated that the untreated surface water samples' mean TDS and EC values (ERWA and EBRW) were lower than those for groundwater (FBW and ABW) during the rainy season. This could result from dissolved solid mineral contents in the aquifer of these study areas [23, 24, 25]. During the dry season, both the surface and groundwater samples were noted to have mean values higher than their corresponding values during

the rainy season. This trend has been attributed to the dilution of the ions by rainwater by many researchers [36]. After the treatment of the water samples during both seasons, the mean values of the TDS and EC were found to reduce. The mean values obtained were all within the allowable range of the (World Health Organization [WHO] [37] and Standard Organization of Nigeria [SON] [38]). This shows that the composite materials used were effective in reducing the values. All the pH values of the untreated and treated water samples during both seasons were alkaline and slightly acidic. The slight increase in the mean pH values of the surface water samples during the dry season may be traced to human activities, such as laundry, around the River (Fonddriest Environmental, Inc [FEI] [39]). Generally, the pHs of the treated water samples were all lower than their corresponding untreated samples. This may result from the decreasing pH nature of ISC [40].

3.2. Effect of surface charge and physicochemical characteristics

Figure 1 displays the points of zero charge (pHpzc) for GCSC, ACSC, and the generated iron(III) sulphate coagulant. GCSC and ACSC had pHpzc values of 7.32 and 7.12, respectively, whereas the ISC had a pHpzc of 2.92. Figure 1 shows that at pH 7.32 and 7.12, the net charge on the surface of both adsorbents was equal to zero. Therefore, when the pH of the solution is below these values, i.e.,

Table 2. Mean Values of Physicochemical Parameters of the Untreated and Treated Water Samples during the Rainy and Dry Seasons

Parameter	Sample	Rainy Season		Dry Season	
		Untreated Mean \pm Std	Treated Mean \pm Std	Untreated Mean \pm Std	Treated Mean \pm Std
TDS (mg L ⁻¹)	ERWA	15.60 \pm 0.13	5.20 \pm 0.14	20.52 \pm 0.74	2.11 \pm 0.46
	EBRW	10.17 \pm 0.52	4.46 \pm 0.37	16.18 \pm 0.12	0.88 \pm 0.23
	FBW	43.05 \pm 0.17	31.73 \pm 0.22	72.61 \pm 0.20	5.35 \pm 0.05
	ABW	30.33 \pm 0.18	27.25 \pm 0.20	51.48 \pm 0.17	1.25 \pm 0.20
EC (μ S cm ⁻¹)	ERWA	98.44 \pm 0.35	67.72 \pm 0.44	146.58 \pm 0.88	38.22 \pm 0.34
	EBRW	58.63 \pm 0.18	27.86 \pm 0.52	93.56 \pm 0.14	16.75 \pm 0.08
	FBW	113.55 \pm 0.11	84.90 \pm 0.30	206.41 \pm 0.16	41.62 \pm 0.09
	ABW	69.89 \pm 0.14	62.07 \pm 0.18	100.02 \pm 0.22	30.76 \pm 0.41
pH	ERWA	6.84 \pm 0.07	6.68 \pm 0.10	7.66 \pm 0.18	6.94 \pm 0.26
	EBRW	7.02 \pm 0.16	6.70 \pm 0.14	7.54 \pm 0.19	7.16 \pm 0.24
	FBW	7.97 \pm 0.08	7.05 \pm 0.05	8.05 \pm 0.12	7.42 \pm 0.25
	ABW	8.01 \pm 0.16	7.64 \pm 0.08	7.57 \pm 0.30	6.72 \pm 0.27

if the solution is acidic, the hydrogen ions in the solution bind with the surface functional groups of the adsorbent, creating a positive charge on the adsorbent surface. This development will hence facilitate the adsorption of anions in the solution. However, if the pH of the solution is above the pH_{pzc} of the adsorbent, the surface functional groups will lose protons, thereby making the adsorbent's surface negatively charged. This will enhance the adsorption of cations such as dissolved heavy metals by electrostatic attraction [41]. On the other hand, the alkaline nature of the water samples resulted in the precipitations of the heavy metal ions as hydroxides, which were swept down by the settling coagulant flocs, resulting in the removal of the dissolved heavy metals. Nanographene oxide nanomagnetic composite for removal of aluminum in wastewaters, water samples, and Al precipitations have occurred as aluminum hydroxide at basic pH [42].

3.3. Physical surface structures of the granulated activated biomaterials

Figures 2a-f illustrate the results of the GCSC and ACSC morphologies. Figures 2a- c Scanning electron micrographs of granulated coconut shell carbon at 8000, 9000, and 10,000 magnifications showing few micropores with non-uniform mesopores. Figures

2d- f Scanning electron micrographs of apparatus counter softwood carbon at 8000, 9000, and 10,000 magnifications show a flaky, honeycomb-like surface with many micropore distributions. The SEM at 8 000, 9 000, and 10 000 magnifications was employed to view the morphologies and pore structures/distribution on the surfaces of the GCSC and ACSC. It was observed that there were few micropores on the surface of GCSC in addition to non-uniform larger pores (mesopores and pore channels-macropores). The larger pore cavities observed may have resulted from high activation temperature, which led to the conversion of already formed micropores to mesopores and macropores [34], and hence, smaller surface area. [33] attributed this to the evolution of oxygen functional groups of the activated carbon. Figures 2d-f showed the pore structure and distribution of ACSC magnified at 9,000 and 10,000. It was found that the surface was flaky and honeycomb-like, with many micropore distributions, resulting in a larger surface area. The increased pore network and volumes may be attributed to the dehydrating action of NaCl and escaping Na^+ and Cl^- during the activation process, as posited by [33] in Equation 3.

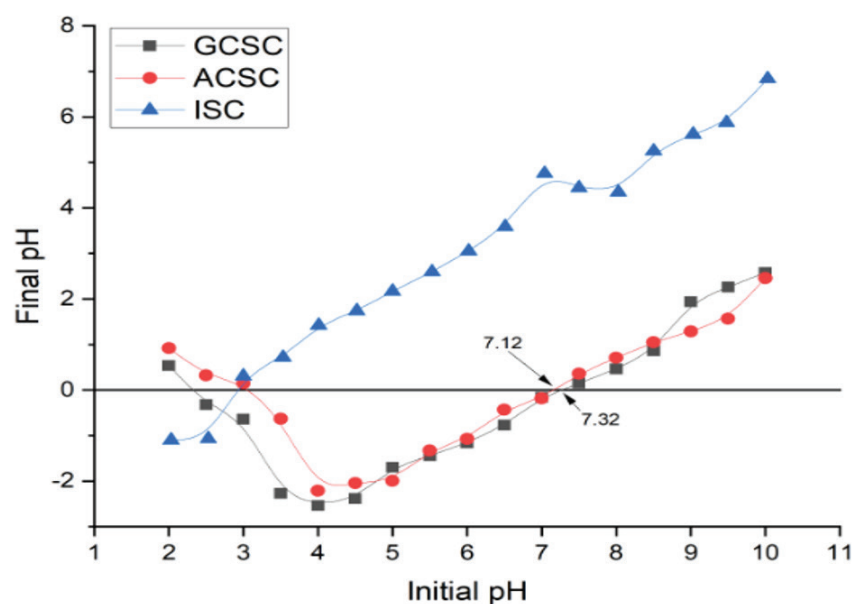
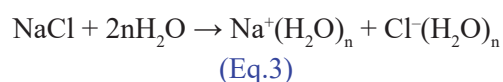


Fig. 1. Points of Zero Charge (pH_{pzc}) for ISC, GCSC and ACSC

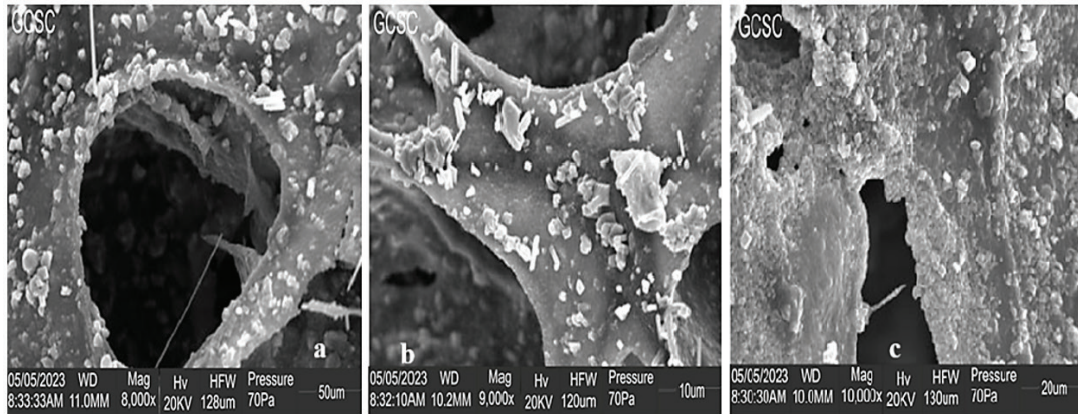


Fig. 2 (a, b, and c). Scanning Electron Micrographs of the GCSC

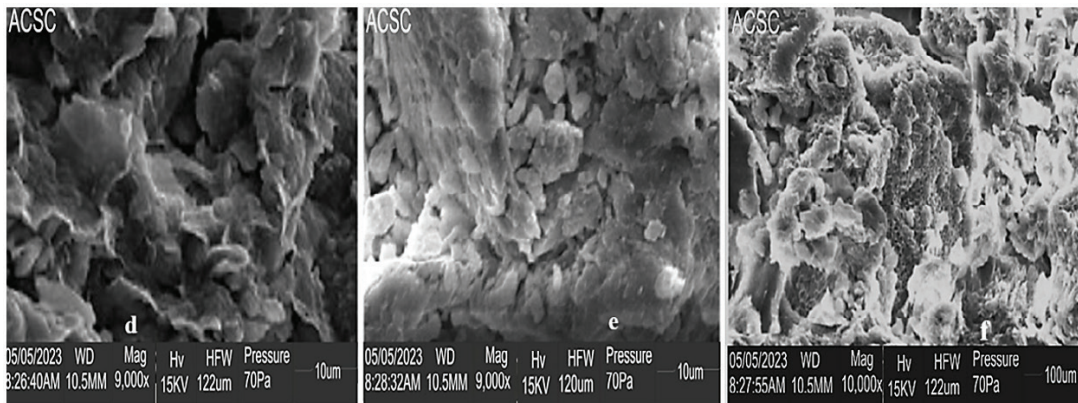


Fig. 2 (d, e, and f). Scanning Electron Micrographs of the ACSC

3.4. Ultimate analysis of GCSC and ACSC

The results for assessing the elemental compositions of the activated GCSC and ACSC are presented in [Figure 3 \(a and b\)](#). The results showed that GCSC contains Cl, C, Na, Si, S, O, N, and Fe, while ACSC contains Cl, C, Na,

Si, S, O, N, and Zn. Carbon has the highest percentage composition, while chlorine was observed to have the lowest percentage composition in GCSC. On the other hand, silicon was the most abundant in ACSC, while zinc had the lowest percentage composition.

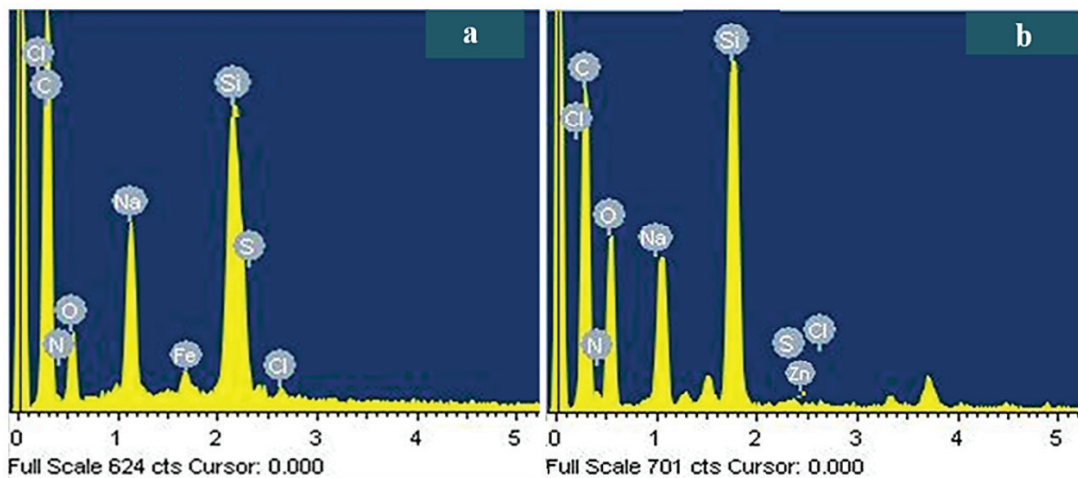


Fig. 3. Energy Dispersive X-ray of GCSC and ACSC (Left side, a): Energy dispersive x-ray of granulated coconut shell carbon indicating that it contained elements such as Cl, C, Na, Si, S, O, N, and Fe, (Right side, b): Energy dispersive x-ray of *akparata* counter softwood carbon showing the composition of Cl, C, Na, Si, S, O, N, and Zn.

3.5. Effect of dose optimization of the composite materials

Table 3 presents the experimental design, indicating the process variables and observed responses for the dosage optimization of composite materials using FBW samples. The initial amounts of Pb, Zn, Cd, and Cu in the FBW sample were 0.205, 0.148, 0.068, and 0.078 mg L⁻¹, respectively. Hence, 0.5, 1.5, and 0.025 g of GCSC, ACSC, and ISC, respectively, were the best dosages of composite materials for achieving the maximum percentage of heavy metals removal.

It is to be noted, however, that the efficiency of removal of the DHMs by the blended composite treatment materials may be affected by the seasonal variations in the pH and temperature of the water samples. Studies have shown that the temperature of the water is affected by many factors, including air temperature and discharges (domestic and industrial) into the water body [43]. In this present study, it was observed that anthropogenic activities (bathing and laundry) were higher during the dry season than the rainy season as the volume of the river waters got reduced (became shallow) due to evaporation, vis-à-vis, increase in air temperature. As expected, the pH of water bodies may rise or fall if there is an increase in the water temperature. An increase in temperature usually stimulates phytoplankton photosynthetic activity, causing more carbon dioxide consumption, which increases pH [44]. Conversely, at higher water temperatures, there is low diffusion of gases, which causes microorganisms to decompose organic matter in the water by anaerobic means, which introduces more CO₂ in the water, resulting in low pH. Therefore, the pH of water bodies may correlate inversely or directly with temperature, depending on other factors. In this present study (Table 1), it was observed that there was a slight increase in the average pH of all

the water samples during the dry season against the average pH recorded for all the water samples during the rainy season. Table 4 and Table 5 presented the results of the percent removal of the DHMs from the various water samples during rainy and dry seasons, respectively. Pb had the highest mean concentrations in all the untreated water samples during the rainy season, while the mean concentrations of Cu and Zn were the least observed in FBW and ABW, EBRW, and ERWA samples, respectively, after treatment. Furthermore, the average levels of dissolved Pb and Cd in untreated FBW, ABW, EBRW, and ERWA samples exceeded the World Health Organization, 2004 according to [39] maximum acceptable limits of 0.01 and 0.003 mg/L, respectively, for drinking water, while the mean concentration of Zn in the EBRW sample exceeded the maximum allowable limits of 3.0-5.0. The mean amounts of the examined dissolved heavy metals in all water samples were below the Regulatory Bodies' recommended limits throughout the dry season. FBW, ERWA, EBRW, and ERWA had the highest % removal of dissolved Cu, Zn, Pb, and Cd during the rainy season, whereas FBW, EBRW, ERWA, and ABW had the lowest percentage removal of dissolved Cu, Zn, Pb, and Cd during the rainy season. The observed trend in the degree of removal was consistent with other previous studies, and this might be explained by Cu and Zn strong attachment to the active sites or pores of the modified biomaterials due to the effective cationic radius [45]. Pb, Cd, Zn, and Cu have effective ionic radius of 0.2655, 0.2305, 0.2165, and 0.2065 nm, respectively [46]. Speciation of lead in human samples based on MWCNTs@DMP was obtained by the ionic liquid-suspension-micro-solid phase [47]. According to [48], heavy metal removal could also be due to initial metal ion concentrations, which

Table 3. Experimental Design Showing the Process Variables and Observed Responses

Run	GCSC	ACSC	ISC	Cu	Zn	Cd	Pd
1	0.500	0.500	0.005	33.330	24.320	38.240	40.980
2	0.500	1.000	0.010	65.390	50.000	77.940	67.810
3	1.000	0.500	0.015	89.740	93.240	88.240	77.560
4	1.500	0.500	0.020	96.150	95.960	88.240	85.370
5	0.500	1.500	0.025	97.440	98.650	88.240	89.760
6	2.000	2.000	0.030	93.590	97.300	88.240	85.850

is the driving force to overcome all mass transfer resistance of metal between the aqueous and solid phases. However, as the prevailing pH of the solutions increased, the adsorption of the DHMs increased. The level of dissolved DHMs in untreated water samples was below the detection limits of the instrument used during the dry season. After treatment, 100 percent removal of the detected dissolved components was achieved in the FBW, ABW, and EBRW samples. Though some of the water samples were alkaline and could have antagonized the effective adsorption of the DHMs by the GACSC [48], however, the ISC which is acidic in nature lowered the pH of the solution and enabled the removal (adsorption and coagulation) of the heavy metals from the water samples. Tables 4 and 5 indicated that during the rainy season, the efficiency of removal of the DHMs followed the order Zn>Cu>Pb>Cd for FBW, ABW, and ERWA samples, while during the dry season, the efficiency of removal was in the order Zn=Cu=Pb in all the samples. Furthermore, the river waters were slightly more alkaline during the dry season in the present study due to increased water temperature necessitating increased photosynthesis by aquatic plants. The efficiency of removal of the DHMs

depends on many factors, including the surface chemistry of the modified biomaterial and the pH range upon which the iron(III) floc (amorphous hydroxide) remains stable. At low pH, there is competition for adsorption of available sites between the DHMs and protons, resulting in lower removal efficiency. As pH increases, there is deprotonation on the surface of the modified biomaterials, causing the surface to be negatively charged and, hence, increasing removal efficiency. On the other hand, it has been revealed that the soluble monomeric hydrolytic species of Fe(III) in equilibrium with the amorphous hydroxide occur over a wider pH range (4.0 –10.0). The solubility of amorphous species, Fe(OH)₃, is least at pH 4 but increases to its plateau at pH 9 and then steeply above pH 9 [49]. Furthermore, an increase in the temperature of the aqueous solution has been revealed to result in an increase in the efficiency of coagulants [30]. Therefore, it might be reasonable to posit in the present study that the removal efficiency of the DHMs by the blended composite treatment materials was enhanced as the temperature and pH of the water samples increased during the dry season. This is in tandem with many other findings [50].

Table 4. Degree of Removal of Dissolved Heavy Metals in Water Samples during Rainy Season

Sample	Metals	Initial pH	Untreated Mean Conc. (mg L ⁻¹)	Treated Mean Conc. (mg L ⁻¹)	% Rm Permissible Limit
FBW	Pb	7.97	0.205 ± 0.021	0.021 ± 0.002	89.76
	Zn		0.148 ± 0.015	0.005 ± 0.001	96.62
	Cd		0.068 ± 0.007	0.012 ± 0.001	82.35
	Cu		0.078 ± 0.008	0.121 ± 0.001	97.44
ABW	Pb	8.01	0.161 ± 0.016	0.010 ± 0.001	93.79
	Zn		0.109 ± 0.011	0.002 ± 0.000	98.17
	Cd		0.026 ± 0.003	0.006 ± 0.001	76.92
	Cu		0.096 ± 0.009	0.005 ± 0.001	94.79
EBRW	Pb	7.02	1.371 ± 0.053	0.011 ± 0.001	99.19
	Zn		11.153 ± 0.643	4.220 ± 0.342	62.16
	Cd		0.044 ± 0.002	0.008 ± 0.000	81.81
	Cu		0.101 ± 0.004	0.006 ± 0.000	94.06
ERWA	Pb	6.84	0.100 ± 0.002	0.018 ± 0.001	82.00
	Zn		0.099 ± 0.005	0.002 ± 0.000	97.98
	Cd		0.023 ± 0.002	0.004 ± 0.000	82.60
	Cu		0.042 ± 0.003	0.005 ± 0.001	88.10

Where ND represents not detected

WHO and SON Maximum(n=3): Pb=0.01, Zn=3.0-5.0, Cd=0.003, Cu=1.0

Table 5. Degree of Removal of Dissolved Heavy Metals in Water Samples during Dry Season

Sample	Metals	Initial pH	Untreated Mean Conc. (mg L ⁻¹)	Treated Mean Conc. (mg L ⁻¹)	% Rm Permissible Limit
FBW	Pb	8.05	0.701 ± 0.032	ND	100
	Zn		0.143 ± 0.006	ND	100
	Cd		ND	ND	ND
	Cu		0.230 ± 0.012	ND	100
ABW	Pb	7.57	ND	ND	ND
	Zn		0.101 ± 0.005	ND	100
	Cd		ND	ND	ND
	Cu		ND	ND	ND
EBRW	Pb	7.54	0.100 ± 0.004	ND	100
	Zn		ND	ND	ND
	Cd		ND	ND	ND
	Cu		0.101 ± 0.005	ND	100
ERWA	Pb	7.66	ND	ND	ND
	Zn		ND	ND	ND
	Cd		ND	ND	ND
	Cu		ND	ND	ND

Where ND represents not detected

WHO and SON Maximum(n=3): Pb=0.01, Zn=3.0-5.0, Cd=0.003, Cu=1.0

3.5.1. Statistical relevance of the optimization process

The statistical relevance of the optimization process of the composite materials for the removal of the DHMs in the FBW sample was carried out using a reduced linear model of analysis of variance (ANOVA) as shown in Table 6. There was evidence that the model was suitable and statistically significant in describing the experimental data based on their probability >F values being less than 0.05 except for the percent removal of Cd where the probability >F values were greater than 0.05. The probability>F values showed that the ISC component of the composite had a much-pronounced effect on the percent removal of Cu, Cd, and Pb, while ACSC and GCSC contributed

latently in influencing the percent removal of the DHMs. This apparent non-contribution by the GCSC and ACSC to the removal of the DHMs was attributed to the reduced linear model used, which does not imply that the adsorbents did not entirely have an effect on the removal of the DHMs.

The relevance of the reduced linear model in describing the experimental data was collaborated by the plot of predicted percent removal of DHMs from the model against actual or experimental percent removal of DHMs in Fig 4 (a to d). For removing Cu, Zn, Cd, and Pb, the determination coefficient (R²) values were 0.7202, 0.9147, 0.5636, and 0.7654, respectively. These values indicated that the regression model did not capture 0.2798, 0.0853, 0.4364, and 0.2346 % of the total

Table 6. F-values and Prob >F from analysis of Variance for the Reduced Linear Model

Response	Cu		Zn		Cd		Pb	
	F-value	Prob>F	F-value	Prob>F	F-value	Prob>F	F-value	Prob>F
RL	10.32	0.0325	16.09	0.0249	5.17	0.0855	13.05	0.0225
ISC	10.32	0.0325	26.60	0.0141	5.17	0.0855	13.05	0.0225
ACSC	----	----	5.71	0.0968	----	----	----	----
Removal %	97.440		98.650		88.240		89.760	

RL: Reduced Linear

possible variations. Furthermore, the adjusted determination coefficients (R^2_a) for the various heavy metals, CuR^2_a (0.6509), ZnR^2_a (0.8579), CdR^2_a (0.4545), and PbR^2_a (0.7068), were of high linear relationship for Zn and Pb, moderate for Cu but was weak for Cd. R^2_a adjusts the R^2 for the regression model's sample size and number of variables. Figure 4a shows the plot of the predicted percent removal of Cu against the experimental percent with a square of regression of 0.7202. Figure 4b plots the expected percent removal of Zn against the experimental percent with a square of regression of 0.0853. Figure 4c is a plot of the predicted percent removal of Cd against the experimental percent with the square of regression of 0.5636. Figure 4d plots the predicted percent removal of Pb against the experimental percent with a square of regression of 0.7654.

To predict both the main and interaction effects in this study, it was necessary to use a 3D response surface plot and the corresponding x/y 2D contour plot on the response variables. The response surface plots showing the effects of the experimental

variables on the percent removal of Cu, Zn, Cd, and Pb in the ABW sample were presented in Figures 5, 6, 7, and 8, respectively. Figure 5a shows the main and interaction effects of ISC and ACSC on the percent removal of Cu while keeping GCSC constant. It was observed from the plot that irrespective of the incremental amount of ACSC, there was no influence on the percentage of dissolved Cu removed. Nevertheless, there was a positive correlation between the amount of ICS used and the percentage of dissolved Cu removed. The same trend was observed in Figure 5b for the main and interaction effects of ISC and GCSC on the percent removal of Cu while keeping the amounts of ACSC constant. The main and interaction effects of the amounts of GCSC and ACSC on the percent removal of Zn while keeping the amounts of ISC steady are shown in Figure 6a. The amounts of ACSC used varied directly with the percent removal of Zn, though minimally. In contrast, the effect of the GCSC on the percent removal of Zn remained constant, irrespective of the increment in amounts. There was a positive correlation between ACSC and the

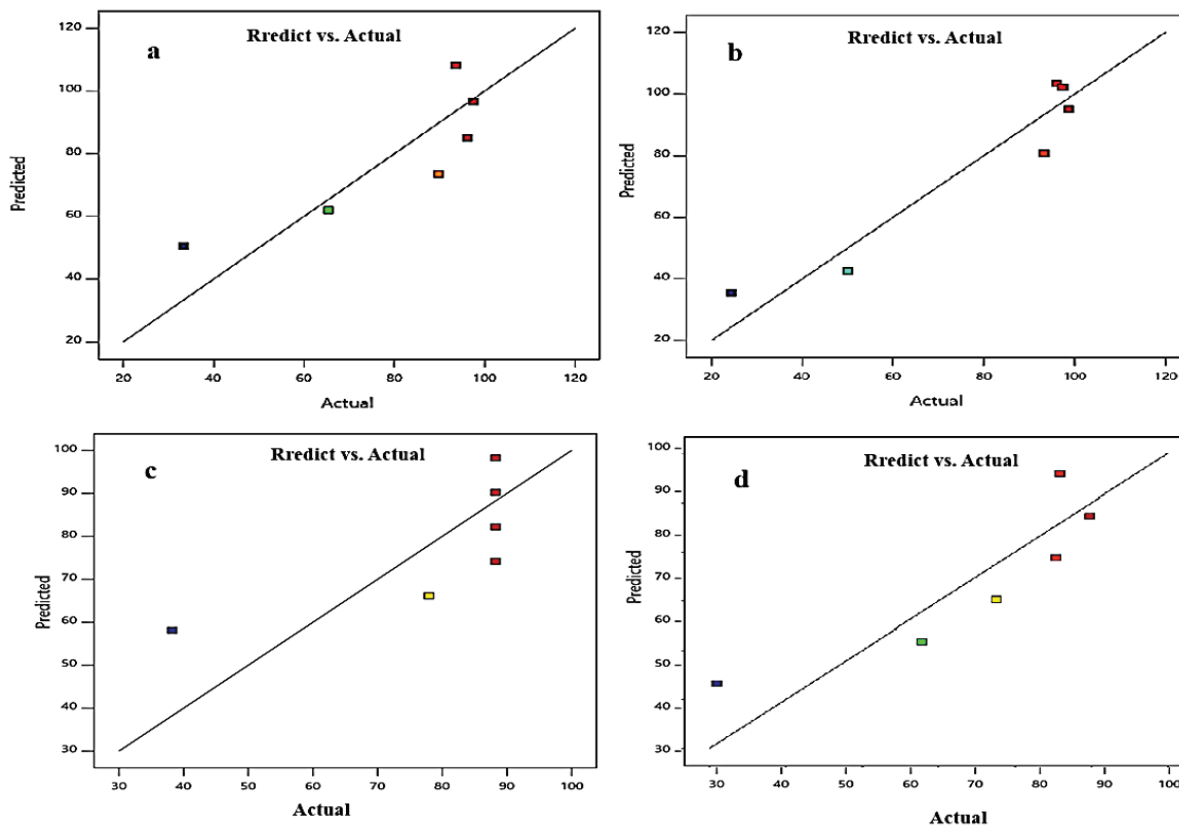


Fig. 4 a – 4d. Plots of Predicted against Actual Values for Percent Removal of Cu, Zn, Cd, and Pb, respectively.

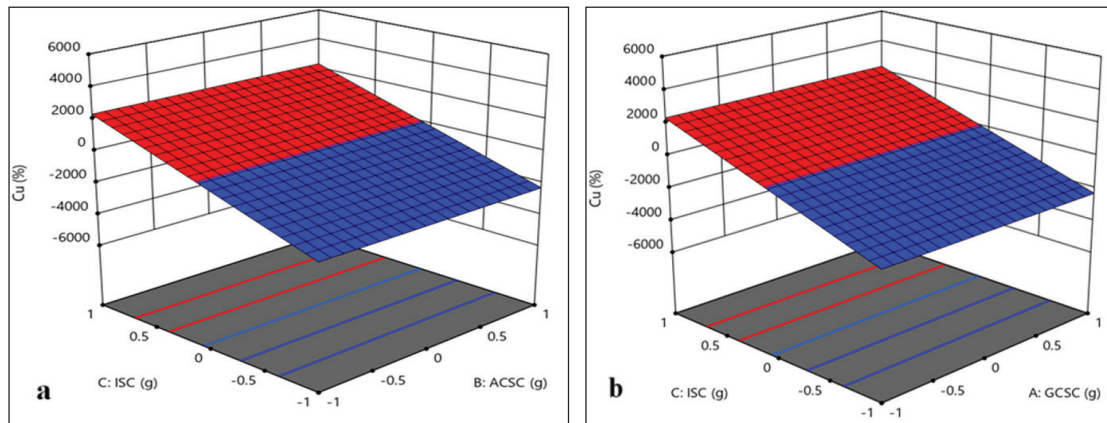


Fig. 5. a) Main Interaction and Effects of ISC and **b)** ACSC, and ISC and GCSC on the Percent Removal of Cu.

percent removal of Zn, while GCSC did not show a positive correlation. Figure 6b revealed that ISC had a significant positive correlation with the percent removal of Zn, while ACSC had no influence on the removal of Zn. Figure 6c shows a positive correlation between ISC and the percent removal of Zn. On keeping the amounts of GCSC constant, Figure 6b shows the main and interaction effects of the amounts of ACSC and ISC on the percent

removal of Zn. Compared to the observation in Figure 6a, ISC had a more significant influence on the percent removal of Zn than the removal of Cu, while ACSC had no effect on the percent removal of Zn. The same trend was observed in Figure 6c when the impact of ACSC was kept constant, and the main and interaction effects of ISC and GCSC on the percent removal of Zn were investigated. Figures 7a and 7b show the main and interaction

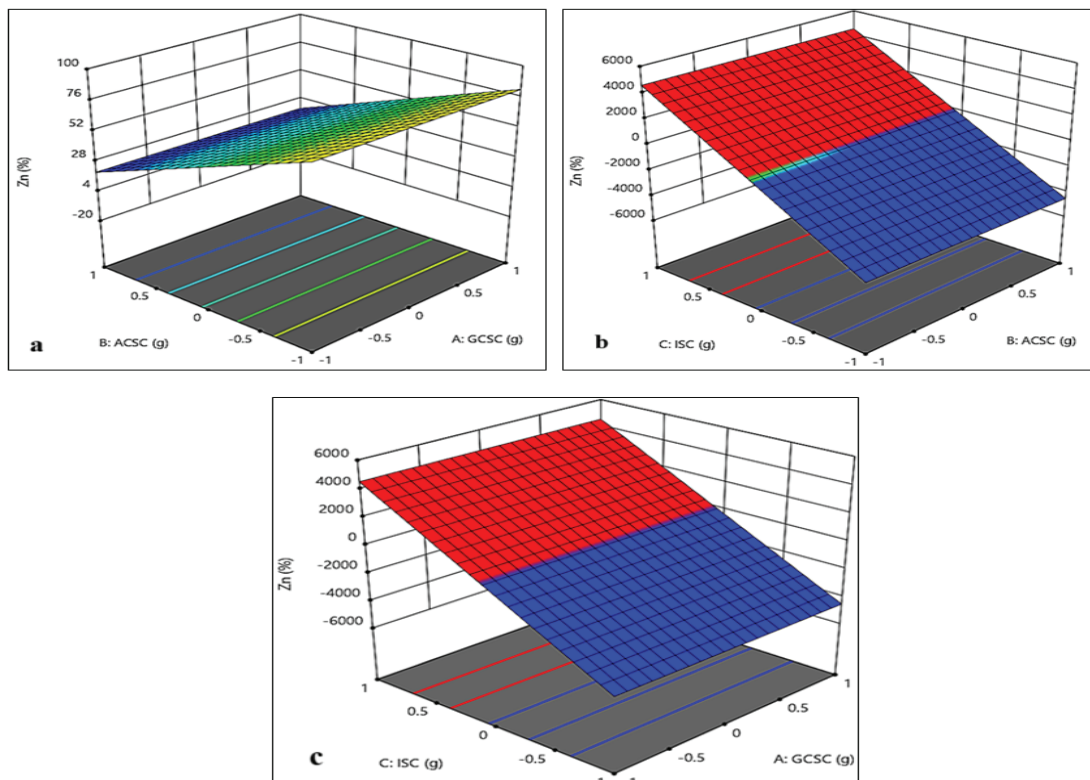


Fig. 6. a) Main Interaction and Effects of ACSC and GCSC, **b)** ISC and ACSC, and **c)** GCSC on the Percent Removal of Zn.

influences of the amounts of ISC and ACSC, ISC and GCSC on the percent removal of Cd while keeping the effects of the amounts of GCSC and ACSC steady, respectively. Both plots showed the same trend: only the ISC had moderate positive correlations with the percent of Cd removed from the FBW sample.

Figures 8a and b present the response surface plots for the primary and interaction effects of ISC and GCSC and ISC and ACSC on the percent removal of Pb while maintaining the amounts of ACSC and GCSC constant, respectively. Figures 8a and b revealed that the ISC varied directly with the percent removal of Pb, while the GCSC and ACSC had no relationship with this. There are two response surface plots in which Figure 8a shows the interaction between GCSC and ISC, with a positive correlation between ISC and the percent removal of Pb. Figure 8b shows the interaction between ACSC and ISC in which a positive correlation existed between ISC and the percent removal of Pb.

3.5.2. Statistical Analysis of the Mean Levels of DHMs in Treated Water Samples

Table 7 presented the result for testing the season's significance, untreated/treated water samples, and metals in removing dissolved heavy metals.

At the conventional 5 % level of significance, there was evidence of significant difference ($p < 0.05$) only in the means of the two seasons. However, at a 10 % level of significance, there was evidence of a significant difference ($p < 0.1$) in the degree of removal of heavy metals between the untreated and treated water samples. This implies that the composite materials used were synergetic in removing heavy metals. None of the various samples and metals showed evidence of a significant mean difference in the degree of removal of dissolved heavy metals. This may result from the surface water and groundwater samples during both seasons experiencing the same technique of heavy metals removal. With mean values of 0.006 and 0.0135, the removal of heavy metals seems higher during the dry season and for treated water, respectively. Even though no significant evidence was established for both the samples and metals, the degree of heavy metal removal appears higher for ERWA and lower for EBRW. This may be attributed to the initial concentrations of the heavy metals in the two River samples. In the same way, removal was also higher with samples containing Cd and lowest with water samples containing Zn.

Table 8 shows the interactions between the DHMs

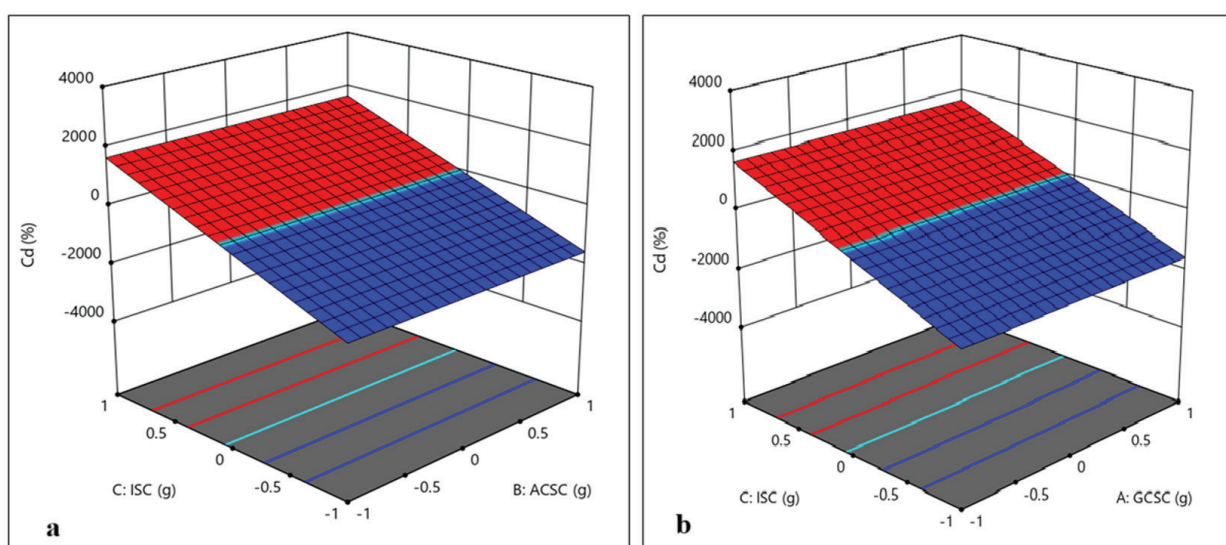


Fig. 7. Main Interaction and Effects of ACSC and GCSC on ISC, a) ACSC vs. ISC and b) GCSC vs. ISC for Removal of Cadmium

and the water samples. The interest was to investigate if all possible interaction effects of metals and water samples produced the same degree of removal. Generally, at as small as a 1 % significance level, there was evidence of a significant ($p < 0.01$) mean difference in the degree of heavy metal removal for all the possible interactions. At a 1 % level of

significance, the variable interactions showed that Zn demonstrated higher interactions with the samples by having the highest mean values. Pb, Cu, and Cd followed this in a decreasing order of mean values. Cd-ERWA produced the highest degree of heavy metal removal, followed by Cd-ABW, Cu-ERWA, and so on, while removal was lowest in Zn-

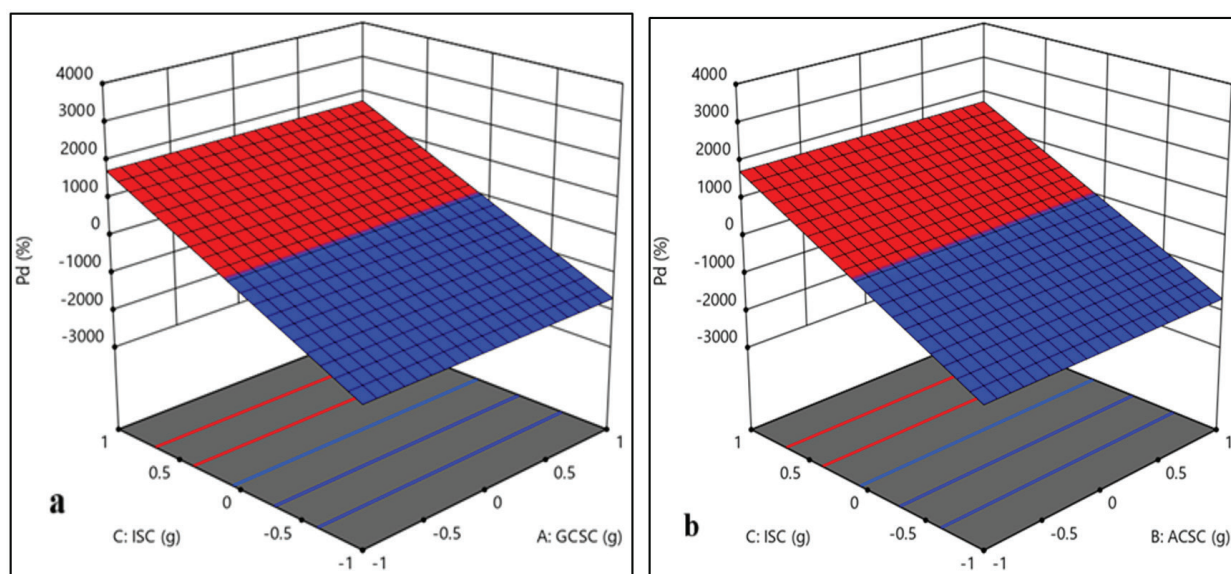


Fig. 8. Main Interaction and Effects of ISC and GCSC, and ISC and ACSC on the Percent Removal of Lead (Pb)

Table 7. Test of Significance: season, untreated/treated water samples, water, and metals in removing dissolved heavy metals

Factors	Variables	Mean sd	Sig. value ($p < 0.05$)
Season	Rainy	0.567 ± 0.028	0.001
	Dry	0.006 ± 0.000	
Water	Untreated	0.438 ± 0.011	0.072
	Treated	0.135 ± 0.005	
Samples	FBW	0.044 ± 0.002	0.354
	ABW	0.027 ± 0.001	
	EBRW	1.057 ± 0.055	
	ERWA	0.018 ± 0.001	
Metal	Pb	0.118 ± 0.005	0.419
	Zn	0.993 ± 0.045	
	Cd	0.012 ± 0.000	
	Cu	0.022 ± 0.001	

EBRW. It can also be observed that interaction with ERWA produced a high degree of removal for each of the four metals. In contrast, most metal interactions with EBRW resulted in a low degree of removal. This observation in this work implied that there were different factors (i.e., pH, initial cation concentrations in the multi-metal system, effective ionic radius, etc.) responsible for removing heavy metals from the individual water samples for both seasons. This was in line with the investigations of [45, 47, 48].

Table 9 shows the multivariate test for the factors (season, water, samples, and metal) and their corresponding variables at 1, 5, and 10 % levels of significance. It was used to check for evidence of a significant mean difference between vector means relating to two groups. Concentrations 1, 2, and 3 were considered independent variables. At the 1 % significance level, there was evidence of a significant difference in means for samples, whereas the season was not substantial; water and metal at 1 %, 5 %, and

even as high as 10 % were insignificant. This showed that with the observations made independently at three concentrations, heavy metal removal patterns were not the same for the samples.

Table 10 presented the result for testing the significant mean difference in the degree of heavy metal removal for both rainy and dry seasons. Table 10 revealed significant values of the variables during the rainy and dry seasons, which ranged from <0.001 to 0.002 and <0.001 to 0.004, respectively. For both seasons, there was evidence of a significant difference ($p < 0.05$) in the degree of removal of heavy metals for treated and untreated water. Whereas the degree of removal is high for treated water, the dry season seems to present a tendency for a higher removal of heavy metals. Lower concentrations of the DHM in water samples during the dry season contributed to this, as evidenced by the lower mean values across all samples and metals.

Table 11 shows the result of the investigation

Table 8. Metal-sample interaction between the DHMs and the water samples

Variable Interaction		Mean sd	Sig. value
Cu	FBW	0.026	<0.001
	ABW	0.025	<0.001
	EBRW	0.027	<0.001
	ERWA	0.012	<0.001
Zn	FBW	0.074	<0.001
	ABW	0.030	<0.001
	EBRW	3.843	<0.001
	ERWA	0.025	<0.001
Cd	FBW	0.020	<0.001
	ABW	0.008	<0.001
	EBRW	0.013	<0.001
	ERWA	0.007	<0.001
Pb	FBW	0.056	<0.001
	ABW	0.043	<0.001
	EBRW	0.345	<0.001
	ERWA	0.027	<0.001

Table 9. Multivariate Hotelling's Test, Concentrations 1, 2, and 3 were considered independent variables

Factor	Variable	Conc..	Sig. value
Season	Rainy	0.567 ± 0.024	0.116
	Dry	0.006 ± 0.001	
Water	Untreated	0.438 ± 0.024	0.393
	Treated	0.135 ± 0.006	
Sample	FBW	0.044 ± 0.002	0.107
	ABW	0.027 ± 0.001	
	EBRW	1.057 ± 0.051	
	ERWA	0.018 ± 0.011	
Metal	Pb	0.118 ± 0.005	0.156
	Zn	0.993 ± 0.045	
	Cd	0.012 ± 0.001	
	Cu	0.022 ± 0.001	

Table 10. Test of Significance during the rainy and dry seasons

Factors	Variables	Mean sd	Sig. value	Mean sd	Sig. value
		Rainy Season		Dry Season	
Water	Untreated	0.864 ± 0.043	0.002	0.012 ± 0.001	0.004
	Treated	0.270 ± 0.013		ND	
Samples	FBW	0.066 ± 0.003	<0.001	0.022 ± 0.002	<0.001
	ABW	0.052 ± 0.002		ND	
	EBRW	2.114 ± 0.107		ND	
	ERWA	0.035 ± 0.001		ND	
Metals	Pb	0.235 ± 0.012	<0.001	ND	0.002
	Zn	1.967 ± 0.112		0.019 ± 0.001	
	Cd	0.024 ± 0.001		ND	
	Cu	0.042 ± 0.002		ND	

to ascertain whether there was an increment or reduction in the DHMs removal due to the interaction of each of the metals with all the water samples during both seasons. The interactions of the heavy metals with the samples during rainy season in the order of decreasing removal was as follows: Cd-ERWA > Cd-ABW > Cu-ERWA > Cd-EBRW > Cu-FBW > Zn-ERWA > Cu-ABW > Cu-EBRW > Pb-ERWA > Zn-ABW > Zn-FBW > Pb-ABW > Pb-FBW > Pb-EBRW > Zn-EBRW. During dry season, the decreasing order is as follows: Cd-ABW = Cd-EBRW = Cd-ERWA = Cd-FBW = Cu-ABW = Cu-ERWA = Pb-ABW = Pb-EBRW = Pb-ERWA = Pb-FBW = Zn-EBRW = Zn-ERWA > Cu-EBRW > Pb-FBW > Zn-ABW > Cu-FBW > Zn-FBW.

At $p < 0.001$ in the two seasons, there was evidence of a significant difference in the degree of heavy metal removal. Again, the dry season presented evidence of increased removal of heavy metals across all metal-sample interactions. As in the overall case presented in Table 8, Cd-ERWA interaction enabled higher removal, followed by Cd-ABW interaction, then Cu-ERWA interaction,

and so on, down to Zn-EBRW, which had reduced heavy metal removal. Generally, metal interactions with ERWA appeared to encourage high removal of heavy metal, while metal interactions with EBRW lowered the degree of heavy metal removal. The result was in tandem with the initial metal ions concentrations in the untreated water samples (Table 5 and Table 6) and other previous works due to surface saturation [48].

During both seasons, the interaction of heavy metals and treatment materials was presented in Table 12, which showed higher removal in treated samples than in untreated samples. The result also showed evidence of significance between composite treatment materials (i.e., GCSC, ACSC, and ISC), heavy metals, and water samples. A P-value of < 0.001 implied enough evidence of significance in the degree of metal removal concerning treatment materials-metals-samples interaction. Removal was notably high in treated-Cu-FBW, treated-Zn-ABW and treated-Zn-ERWA. This was closely followed by treated Cd-ERWA, while removal was lowest in treated Zn-EBRW.

Table 11. Metal-sample Interaction by Season

Variable Interaction		Mean sd	Sig. Value	Mean sd	Sig. value
		Rainy season		Dry season	
Cu	FBW	0.040 ± 0.002	<0.001	0.011 ± 0.001	<0.001
	ABW	0.051 ± 0.003	<0.001	ND	<0.001
	EBRW	0.053 ± 0.004	<0.001	ND	<0.001
	ERWA	0.024 ± 0.001	<0.001	ND	<0.001
Zn	FBW	0.077 ± 0.008	<0.001	0.072 ± 0.003	<0.001
	ABW	0.055 ± 0.006	<0.001	0.015 ± 0.001	<0.001
	EBRW	7.687 ± 0.256	<0.001	ND	<0.001
	ERWA	0.050 ± 0.004	<0.001	ND	<0.001
Cd	FBW	0.040 ± 0.002	<0.001	ND	<0.001
	ABW	0.016 ± 0.001	<0.001	ND	<0.001
	EBRW	0.026 ± 0.001	<0.001	ND	<0.001
	ERWA	0.014 ± 0.002	<0.001	ND	<0.001
Pb	FBW	0.109 ± 0.005	<0.001	0.013 ± 0.001	<0.001
	ABW	0.086 ± 0.004	<0.001	ND	<0.001
	EBRW	0.690 ± 0.036	<0.001	ND	<0.001
	ERWA	0.054 ± 0.001	<0.001	ND	<0.001

Table 12. Test of Significance for Treatment-Metal-Sample Effect

Treatment	Heavy Metal	FBW	ABW	EBRW	ERWA
Untreated	Pb	0.106	0.081	0.686	0.050
	Zn	1.460	0.060	5.577	0.050
	Cd	0.034	0.013	0.022	0.012
	Cu	0.050	0.048	0.051	0.021
Treated	Pb	0.006	0.005	0.005	0.004
	Zn	0.003	0.001	2.110	0.001
	Cd	0.006	0.035	0.004	0.002
	Cu	0.001	0.003	0.003	0.003
P-value		<0.001	<0.001	<0.001	<0.001

4. Conclusion

The results show that 0.5 g, 1.5 g, and 0.025 g masses of the blended composite were successful in removing DHMs in separate 250 ml water samples during the rainy and dry seasons and determined by ICP-OES, respectively, with 62.16 - 99.19 percent and 100 percent removal efficiency. The statistical relevance of the optimization process of the composite materials for the removal of the DHMs using a reduced linear variance analysis model showed evidence of the model being suitable and statistically significant to describe the experimental data. The probability > F values indicated that the ISC component of the composite had a much-pronounced effect on the percent removal of Cu, Cd, and Pb. At the same time, ACSC and GCSC contributed latently in influencing the percent removal of the DHMs due to the reduced linear model used, and this does not imply that the adsorbents did not entirely have an effect on the removal of the DHMs. Furthermore, at ($p < 0.001$, $p < 0.01$, $p < 0.05$, and $p < 0.1$), there were indications of significant mean differences in the following interactions: individual heavy metals with all the water samples during both seasons: DHMs and water samples, and in the vector mean of the water

samples; between untreated and treated water, between water samples and their vector mean, and between the heavy metals during both seasons; as well as between the rainy and dry seasons, between the untreated and treated water, and in the vector mean of the water samples, respectively. With a p-value of <0.001 , there was a significant mean difference concerning the interaction of treatment materials-metals-samples. It is recommended that a composite of 0.5 g GCSC, 1.5 g ACSC, and 0.025 g ISC be used to treat 250 ml of river or borehole water samples for DHMs removal. Additional research should be conducted to comparatively assess all possible effects of separately treating the water samples with the GCSC, ACSC, and ISC while varying the initial pH of the water samples.

5. Abbreviations

FBW	Funai borehole water
ABW	Assemblies of God church borehole water
EBRW	Ebonyi River water
ERWA	Eziyiaku river water, Akaeze
GCSC	Granulated coconut shell carbon
ACSC	<i>Akparata</i> (counter)softwood carbon
ISC	Iron(III) sulphate coagulant
DHMs	Dissolved heavy metals

6. Acknowledgment

I am grateful to the staff of the International Institute of Tropical Agriculture (IITA), Ibadan - where the dissolved heavy metals were quantified using an inductively coupled mass spectrometer; Department of Chemical Engineering, Ahmadu Bello University, Zaria; for obtaining the surface morphology and the electron dispersive x-ray analysis of the adsorbents. I salute my fellow staff of the Department of Chemistry, Alex Ekwueme Federal University, Ndufu-Alike, for their assistance during this study. The authors hereby disclose that they have no known competing financial interests or personal relationships that could have appeared to influence the work reported in this paper.

7. References

- [1] S. J. Cobbina, A. B. Duwiejuah, R. Quansah, Comparative assessment of heavy metals in drinking water sources in two small-scale mining communities in northern Ghana, Nigeria, *Int. J. Environ. Res. Public Health*, 12 (2015) 10620–10634. <https://doi.org/10.3390/ijerph120910620>
- [2] B.O. Oladunni, A. Tejumade, A.O. Otolurin, Heavy metal contamination of water, soil, and plants around an electronic waste dumpsite, *Pol. J. Environ. Stud.*, 22(2013) 1431-1439. <https://www.pjoes.com/pdf-89108-22967?filename=22967.pdf>
- [3] J. Rakhtshah, H. Shir Khanloo, M. Dehghani Mobarake, Simultaneously speciation and determination of manganese (II) and (VII) ions in water, food, and vegetable samples based on immobilization of N-acetylcysteine on multi-walled carbon nanotubes, *Food Chem.*, 389 (2022) 133124. <https://doi.org/10.1016/j.foodchem.2022.133124>
- [4] J.O. Jeje, K.T. Oladepo, Assessment of heavy metals of boreholes and hand dug wells in Ife North Local Government Area of Osun State, Nigeria. *Int. J. Sci. Technol.*, 3 (2014) 209-214. <https://sciencetechnology.uz/index.php/s>
- [5] J. Rakhtshah, Ultrasound assisted-dispersive-modification solid-phase extraction using task-specific ionic liquid immobilized on multiwall carbon nanotubes for speciation and determination mercury in water samples, *Microchem. J.*, 154 (2020) 104632. <https://doi.org/10.1016/j.microc.2020.104632>
- [6] A. Rouhollahi, Speciation, and determination of trace amount of inorganic arsenic in water, environmental and biological samples, *J. Chin. Chem. Soc.*, 58 (2011) 623-628. <https://doi.org/10.1002/jccs.201190097>
- [7] J.M. Misihairabgwi, K. Abisha, A. Peter, C.J. Colin, P.A. Tanya, N. Ignatius, Adsorption of heavy metals by agroforestry waste derived activated carbons applied to aqueous solutions. *Afr. J. Biotech.*, 13(2014) 1579-1587. <https://doi.org/10.5897/AJB2013.12115>
- [8] S. D. Ahranjani, A lead analysis based on amine-functionalized bimodal mesoporous silica nanoparticles in human biological samples by ultrasound assisted-ionic liquid trap-micro solid phase extraction, *J. Pharm. Biomed. Anal.*, 157 (2018) 1-9. <https://doi.org/10.1016/j.jpba.2018.05.004>
- [9] M. M. Eskandari, B. Kalantari, Dispersive liquid-liquid microextraction based on task-specific ionic liquids for determination and speciation of chromium in human blood, *J. Anal. Chem.*, 70 (2015) 1448-1455. <https://doi.org/10.1134/S1061934815120072>
- [10] O.P. Igboji, J.A. Ayodele, Quality of FADAMA and EBSCA boreholes in Abakaliki, Southeastern Nigeria, *Am. Eur. J. Agri. Environ. Sci.*, 16 (2016) 470-478. <https://doi.org/10.5829/idosi.aejaes.2016.16.3.12841>
- [11] J.N. Edeh, L.E. Udu, M.C. Nwankamma, S.O. Chima, Effects of financial corruption on socio-economic development in Ebonyi State: A study of selected Local Government Areas, *Int. Digit. Org. Sci. Res.*, 4 (2019) 24-41. <https://www.idosr.org/wp-content/uploads/2019/07/IDOSR-JAM-42-24-41-2019-LU-P1.pdf>
- [12] M. Bagheri Hosseinabadi, N. Khanjani, M.D. Mobarake, Neuropsychological effects of long-term occupational exposure to mercury among chloralkali workers, *Work*, 66 (2020) 491-498. <https://doi.org/10.3233/WOR-203194>
- [13] V.C. Ezennubia, A.A. Onunkwo, O. Ozotta,

- Baseline verification of heavy metal distribution in surface water bodies of Okposi and environs, Ohaozara Local Government Area, Ebonyi State, Southeastern Nigeria, *Int. J. Adv. Acad. Res. Sci. Technol. Eng.*, 5 (2019) 82-92. <https://doi.org/10.46654/ij.24889849>
- [14] F. Cheronon, N. Mburu, B. Kakoi, Adsorption of lead, copper and zinc in a multi-metal aqueous solution by waste rubber tires for the design of single batch adsorber, *Heliyon*, 7(2021) e08254. <https://doi.org/10.1016/j.heliyon.2021.e08254>
- [15] F. Golbabaee, Z. Sadeghi, A. Vahid, A. Rashidi, On-line micro column preconcentration system based on amino bimodal mesoporous silica nanoparticles as a novel adsorbent for removal and speciation of chromium (III, VI) in environmental samples, *J. Environ. Health Sci. Eng.*, 13 (2015) 1-12. <https://doi.org/10.1186/s40201-015-0205-z>
- [16] M. D. Mobarake, Ultrasound-assisted solid-liquid trap phase extraction based on functionalized multi-wall carbon nanotubes for preconcentration and separation of nickel in petrochemical waste water, *J. Anal. Chem.*, 74 (2019) 865-876. <https://doi.org/10.1134/S1061934819090090>
- [17] S. Davari, F. Hosseini, Dispersive solid-phase microextraction based on aminefunctionalized bimodal mesoporous silica nanoparticles for separation and determination of calcium ions in chronic kidney disease, *Anal. Methods Environ. Chem. J.*, 1 (2018) 57-66. <https://doi.org/10.24200/amecj.v1.i01.37>
- [18] F. Golbabaee, A. Vahid, A. Faghihi Zarandi, A novel nano-palladium embedded on the mesoporous silica nanoparticles for mercury vapor removal from air by the gas field separation consolidation process, *Appl. Nanosci.*, 12 (2022) 1667-1682. <https://doi.org/10.1007/s13204-022-02366-0>
- [19] I. Andrew-Oha, K. Mosto-Onuoha, S. Sunday-Dada, Contrasting styles of lead-zinc-barium mineralization in the lower Benue trough, Southeastern Nigeria, *Earth Sci. Res. J.*, 21 (2017) 7-16. <https://doi.org/10.15446/esrj.v21n1.39703>
- [20] D. Igwe, J. Afiukwa, F. Nwabue, Seasonal evaluation of total organic carbon removal from river samples using scrap metal-based coagulant and local salt modified-biomaterials for point-of-use water treatment, *Int. J. Environ. Anal. Chem.*, 103 (2021a) 1-21. <https://doi.org/10.1080/030673192021.1875451>
- [21] D.O. Igwe, J.N. Afiukwa, F.I. Nwabue, Evaluation of the anti-microbial efficiency of scrap metal-based coagulant and local salt modified-biomaterial for point-of-use water treatment, *Int. J. Phy. Sci.*, 16 (2021b) 36-51. <https://doi.org/10.5897/IJPS2020.4926>
- [22] J.E. Obarezi, J.I. Nwosu, Structural controls of Pb-Zn mineralization of Enyigba District, Abakaliki, Southeastern Nigeria, *J. Geo. Min. Res.*, 5 (2013) 250-261. <https://doi.org/10.5897/JGMR13.0189>
- [23] O.C. Okeke, E.C. Dioha, I.B. Umeorizu, M.C. Mmerole, N.I. Nwakwasi, Physico-chemical and bacteriological characteristics and quality assessment of groundwater from shallow aquifer in Abakaliki town, Southeastern Nigeria, *Int. J. Adv. Acad. Res. Sci. Technol. Eng.*, 2(12) (2016) 60-73. <https://www.ijaar.org/about-ijaar/>
- [24] M.O. Eyankware, Hydrogeochemical evaluation of groundwater for irrigation purpose in Ekaeru Inyimagu and its Adjoining Area, Ebonyi State, Nigeria, *Discovery*, 65 (2020) 681-694. https://mail.discoveryjournals.org/discovery/current_issue/v56/n298/A4.pdf?
- [25] T.I. Mgbeojedo, L.S. Al-Naimi, Hydrogeochemical and physico-chemical studies of the groundwater within Afikpo and Abakaliki, Southeastern Nigeria, *Geosci.*, 8 (2018) 32-43. <https://doi.org/10.5923/j.geo.20180802.02>
- [26] F.K. Onu, The southern Benue trough and Anambra basin, Southeastern Nigeria: A stratigraphic review, *J. Geo. Environ. Earth Sci. Int.*, 12 (2017) 1-16. <https://doi.org/10.9734/JGEESI/2017/30416>
- [27] F. D. Wilde, Techniques of Water Resources Investigations (TWRI), Preparations for water

- sampling, Book 9 (version 2.0, 1/05), U.S Geological Survey, pp. 1-46, 2004. <https://pubs.usgs.gov/twri/twri9a1/Ch1.pdf>
- [28] B. Mahesh, B. Chandu, B. Sakala, S. Nama, S. Domatoti, Inductively coupled plasma mass spectrometry (ICP-MS), *Int. J. Res. Pharm. Chem.*, 2 (2012) 671-680. <https://doi.org/10.4135/9781446247501.n2037>
- [29] W. Heschel, E. Klose, On the suitability of agricultural by-products for the manufacture of granular activated carbon, *Fuel*, 74 (1995) 1786-1791. [https://doi.org/10.1016/0016-2361\(95\)80009-7](https://doi.org/10.1016/0016-2361(95)80009-7)
- [30] R. Ansari, F.N. Khosbakhhat, Application of polypyrrole coated on wood sawdust for removal of Cr(VI) ion from aqueous solutions, *React. Funct. Polym.*, 67 (2007) 367-374. <https://doi.org/10.1016/j.reactfunctpolym.2007.02.001>
- [31] T. Xiaomin, Z. Huaili, T. Houkai, S. Yongjun, G. Jinsong, X. Wanying, Y. Qingqing, C. Wei, Chemical coagulation process for the removal of heavy metals from water: A review, *Desalin. Water Treat.*, 57 (2016) 1733-1748. <https://doi.org/10.1080/19443994.2014.977959>
- [32] D. Jiang, X. Tianyi, W. Haiyan, Z. Anmin, W. Yong, Effects of cellulose, hemicellulose, and lignin on the structure and morphology of porous carbons, *ACS. Sust. Chem. Eng.*, 4 (2016) 3750-3756 <https://doi.org/10.1021/acssuschemeng.6b00388>
- [33] M. Seri, H. Gewa, A. Irvan, I. Heri, Quality comparison of activated carbon produced from oil palm fronds by chemical activation using sodium carbonate versus sodium chlorid, *J. Korean Wood Sci. Technol.*, 48 (2020) 503-512. <https://doi.org/10.5658/WOOD.2020.48.4.503>
- [34] J. Sahira, K.C. Bishnu, Synthesis and characterization of sugarcane bagasse based activated carbon: Effect of impregnation ratio of ZnCl₂, *J. Nepal Chem. Soc.*, 41 (2020) 74-79. <https://doi.org/10.3126/jnes.v41i1.30490>
- [35] A.J. Nwinyimagu, G.N. Nwonumara, C. Ani, I.O. Ukeje, Evaluation and management of the physicochemical variables of Asu river, Southeast, Nigeria, *J. Sust. Dev.*, 9 (2016) 54-66. <https://doi.org/10.5539/jsd.v9n2p54>
- [36] N. Hannington, B. Denis, N. Emmanuel, Effects of seasonal variations in physical parameters on quality of gravity flow water in Kyanamira Sub-county, Kabale District, Uganda, *J. Water Res. Pro.*, 8 (2016) 1297-1309. <https://doi.org/10.4236/jwarp.2016.813099>
- [37] World Health Organization (WHO), Guideline for drinking water quality fourth Edition incorporating the first addendum, Geneva, 541p, 2017. <https://www.who.int/>
- [38] Standard Organization of Nigeria (SON), Nigeria Industrial Standard for Drinking Water Quality, NIS 977:2017, National Standard for Drinking Water Quality from Standard Organization of Nigeria, 22p, 2017. <https://son.gov.ng/>
- [39] pH of Water, Fundamentals of Environmental Measurements, Fondriest Environmental, Inc., 2013. <http://www.fondriest.com/environmental-measurements/parameters/water-quality/pH>
- [40] J. Bratby, Coagulation and flocculation in water and wastewater treatment (third ed), International Water Association (IWA) Publishing, London, UK, 450 pages, 2006. www.iwapublishing.com
- [41] A.A.O. El-Amin, Removal of resorcinol from aqueous solution by activated carbon: Isotherms, thermodynamics and kinetics, *Am. Chem. Sci. J.*, 16 (2016) 1-13. <https://doi.org/10.9734/ACSJ/2016/27637>
- [42] M. K. Abbasabadi, F. Hosseini, Nanographene oxide modified phenyl methanethiol nanomagnetic composite for rapid separation of aluminum in wastewaters, foods, and vegetable samples by microwave dispersive, *Food Chem.*, 347 (2021) 129042. <https://doi.org/10.1016/j.foodchem.2021.129042>
- [43] S. Haddouta, K.L. Priyab, A.M. Hoguanec, J.C.C. Casilad, I. Ljubenkove, Relationship of salinity, temperature, pH, and transparency to dissolved oxygen in the Bouregreg estuary (Morocco): First results, *Water Pract. Technol.*, 17 (2022) 2654. <https://doi.org/10.2166/wpt.2022.144>
- [44] F. Sinada, M.E. Abdel-Rahman, Water chemistry

- and quality of the white Nile at Khartoum, Sudan
J. Sci., 5 (2013), 1-14. <http://sciencejournal.uofk.edu/>
- [45] K. Roshanak, B.A. Mansor, R.F.M. Hamid, S. Kamyar, B. Mahiran, K. Katayoon, Rapid adsorption of copper (II) and lead (II) by rice straw/Fe₃O₄ nanocomposite: Optimization, equilibrium isotherms, and adsorption kinetics study, *PLOS ONE*, 10 (2015) e0120264. <https://doi.org/10.1371/journal.pone.0120264>
- [46] B. Das, N.K. Mondal, R. Bhaumik, P. Roy, Insight into adsorption equilibrium, kinetics and thermodynamics of lead onto alluvial soil, *Int. J. Environ. Sci. Technol.*, 11 (2014) 1101-1114. <https://doi.org/10.1007/s13762-013-0279-z>
- [47] N. Esmaeili, J. Rakhtshah, E. Kolvari, A. Rashidi, H. Shir Khanloo, Rapid speciation of lead in human blood and urine samples based on MWCNTs@DMP by dispersive ionic liquid-suspension-micro-solid phase extraction, *Biol. Trace Elem. Res.*, 199 (2021) 2496–2507. <https://doi.org/10.1007/s12011-020-02382-7>
- [48] M.N. Saifuddin, P. Kumaran, Removal of heavy metal from industrial wastewater using chitosan coated oil palm shell charcoal, *Electronic J. Biotechnol.*, 8 (2005) 43-53. <https://doi.org/10.4067/S0717-34582005000100008>
- [49] M. K. Abbasabadi, Speciation of cadmium in human blood samples based on Fe₃O₄-supported naphthalene-1-thiol- functionalized graphene oxide nanocomposite by ultrasound-assisted dispersive magnetic micro solid phase extraction, *J. Pharm. Biomed. Anal.*, 189 (2020) 113455. <https://doi.org/10.1016/j.jpba.2020.113455>
- [50] P.W. Olupot, J. Wakatuntu, M. Turyasingura, J. Jjagwe, E. Menya, M. Okure, Optimization of heavy metal removal by activated carbon obtained as a co-product from fast pyrolysis of rice husks, *Results Mater.*, 21 (2024) 100545. <https://doi.org/10.1016/j.rinma.2024.100545>